ON THE RISK OF PERMEABILITY ALTERATION BY SALT PRECIPITATION: AN EXPERIMENTAL INVESTIGATION USING X-RAY RADIOGRAPHY

Souhail Youssef[1], Yannick Peysson[1], Olivier Lopez[2], Jostein Alvestad[2], Christin Weierholt Strandli[2], Øivind Fevang[2]

[1]IFP Energie nouvelles, Rueil-Malmaison, France

[2]STATOIL ASA, Trondheim, Norway

This paper was prepared for presentation at the International Symposium of the Society of Core Analysts held in Vienna, Austria 27 August - 1 September 2017

ABSTRACT

We have experimentally investigated the effect of drying a brine saturated porous medium by gas injection and assessed the resulting salt precipitation on permeability. State of the art equipment designed for high throughput coreflood experimentation was used to capture the dynamics of salt migration. Experiments, where nitrogen gas was injected at an imposed pressure in a brine-saturated core, were monitored by X-ray radiography to visualize the evolution of local saturation and salt concentration as well as salt precipitation. Results show that salt precipitation results from the interplay of different parameters, namely pressure gradient, brine concentration, capillary forces and vapor partial pressure. Experimental observations indicate that in the case of dry gas injection, salt precipitates systematically but permeability alteration is observed only if a capillary contact is maintained with the brine. However, in the case of humid gas injection, presence of brine can inhibit dry-out if an equilibrium is reached between salt concentration and partial vapor pressure.

INTRODUCTION

In the field of natural gas production as well as gas storage in aquifer, salt deposition is considered as a potential risk for gas wells. In Northern Germany, field evidences of mainly halite precipitation have been reported during gas production [1]. A synthetic review of gas well productivity impairment by salt plugging can be found in [2]. Injection of a gas phase through a water saturated porous medium can reduce the water saturation not only by displacement mechanisms but also by evaporation mechanisms. To understand the phenomena of drying induced by gas production, Mahadevan *et al.* [3] did an extensive experimental and theoretical study to show that injection of vapor saturated gas (i.e., humid gas) in a rock sample can induce drying [3-4]. The origin of the drying is that the water mole fraction in the gas phase at equilibrium depends on pressure. In the context of gas storage in aquifer, experiments have been conducted by [5-6] injecting dry gas in brine saturated sandstone samples with different salt concentrations in the brine. They showed that the drying rate is proportional to the gas velocity and that any dissolved salt in the water can be transported by capillary flows induced by drying and can even accumulate near the injection surface. The permeability can then be reduced by pore clogging. They

conclude that all of these mechanisms must be included in models to calculate the near wellbore permeability and porosity changes with time, to correctly determine well injectivity.
In this study, we present a comprehensive experimental investigation of the effect of gas flow in a sandstone sample initially saturated with water or brine. Five experiments have been conducted on a small Bentheimer sandstone sample using different experimental conditions i.e. dry or humid gas, deionized water or brine, with and without capillary contact, in order to highlight the effects of drying by gas injection and salt precipitation on permeability impairment.

MATERIAL AND METHODS

Experiments were conducted on a Bentheimer sandstone of 1 cm in diameter and 2 cm in length with a porosity of 23% and a permeability of 1350 mD. To perform the different experiments, we have used nitrogen, deionized water and a 100 g/l KBr brine. KBr salt was chosen as it has a high electronic density allowing a good X-ray contrast with water. The solubility limit of KBr in water at 20°C is 560 g/l.
The experimental set-up used in this study is shown in Figure 1. Nitrogen was injected at a constant pressure using a downstream pressure regulator. Its flow rate was monitored by a Coriolis mass flow meter. A humidifier canister was used to saturate the gas. Brine solution was injected using an Isco Pump. The different lines were connected to an X-ray transparent hassler type cell equipped from each side with three connections (inlet, outlet and static line for the pressure transducer). A data acquisition system was used to monitor the pressure, mass flow and temperature. Finally, the set-up was installed in a dedicated radiography facility equipment for in-situ saturation monitoring.
During fluid injection, the sample was imaged using an X-ray radiograph equipment. The system consists of an X-ray source, a flat panel and a data processing unit for computation, visualization and data analysis. The radiographs were captured with a resolution a 20 µm at a rate of one frame per second. Radiographs were then cropped to show only the sample (see zone 1 in Figure 1). The stack of images was processed to monitor water saturation and salt concentration evolution during gas injection [7]. Indeed image gray levels are proportional to the transmitted X-ray intensity which is defined by the Beer Lambert's law in the case of a multicomponent material as:

$$I_t = I_o\, e^{-(\mu_{bt} X_b + \mu_g X_g) + \alpha}$$

where I_o and I_t are respectively the incident and the transmitted X-ray intensity, μ_{bt} and μ_g are respectively the brine and the gas attenuation coefficients, X_w and X_g are respectively the brine and the gas portions in the linear path of the X-ray and α is the attenuation of the structure. Considering two references states, 100% brine saturated and dry images the above equation can be written as:

$$I_b = I_o\, e^{-\mu_{b0} X + \alpha} \quad , \quad I_g = I_o\, e^{-\mu_g X + \alpha}$$

where X is the linear path of the X-ray that corresponds to the total porosity and μ_{b0} is the initial brine attenuation coefficient.
By construction we obtain $X_b + X_g = X$

Afterward, normalizing the X-ray intensity I_t by both the 100% brine and the dry case, and considering $\mu_b \gg \mu_g$ we obtain:

$$\frac{\ln\left(\frac{I_b}{I_0}\right) - \ln\left(\frac{I_t}{I_0}\right)}{\ln\left(\frac{I_b}{I_0}\right) - \ln\left(\frac{I_g}{I_0}\right)} = \frac{-\mu_{b0}X + \mu_{bt}X_b}{-\mu_{b0}X}$$

When salt concentration is constant, $\mu_{bt} = \mu_{b0}$ and $\frac{X-X_b}{X} = S_g$, where S_g is the gas saturation. If the salt concentration changes, μ_{bt} will vary with an upper limit equal to the KBr attenuation coefficients. If we normalize the X-ray transmitted intensities (i.e. relative X-ray absorption) by the mean intensity of a dry sample with precipitated salt, we can assess qualitatively the variation of salt quantity compared to the initial distribution.

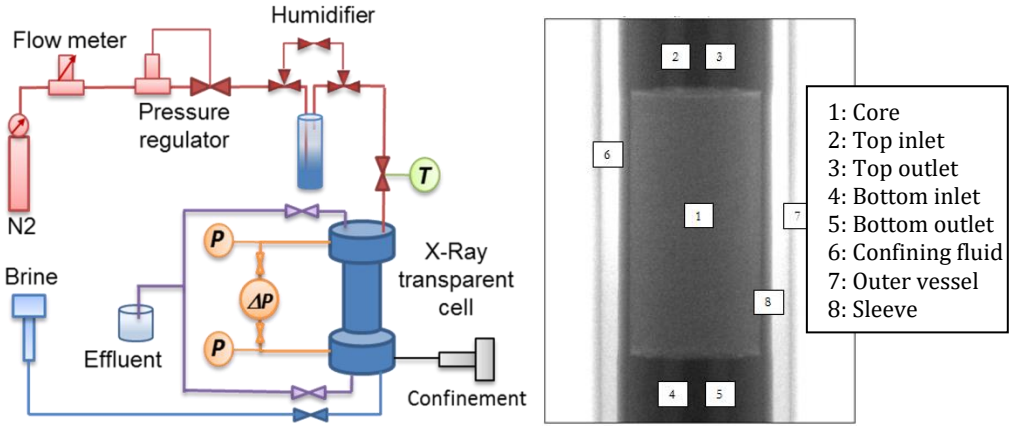

Figure 1: Experimental set-up and a radiograph showing the sample shape and the basic components of the Hassler injection cell.

RESULTS AND DISCUSSION

As pointed out in the introduction, drying and salt precipitation result from the interplay of different parameters. To un-correlate the effect of these parameters, we have conducted a number of experiments that map the parameter domain by varying the gas humidity, salt content and boundary condition (with and without capillary contact). In the following, we discuss the impact of these parameters.

Effect of gas humidity

To study the effect of gas relative humidity, we have conducted two experiments where we have injected dry gas and humid gas, respectively, in a sample initially saturated with deionized water (Experiments 1 and 2). The inlet relative gas pressure was set to 100 mbar. The pressure drop was chosen to be above the entry pressure of 70 mbar and corresponds to a pressure gradient of 5 bar/m which is representative of near well bore pressure gradient. Figure 2 and Figure 4 show the evolution of the mean gas saturation within the sample as well as the mass flow rate of the gas. Four regimes can be distinguished: between 0 and 10 min, the gas drains the sample till a mean residual water saturation of 30% to 40%. Next we observe a smooth increase in the gas saturation and the flow rate until the gas saturation

reaches around 74% (70 min for dry case and 120 min for the humid case). Following this, we note an increase in the gas flow rate as well as in the gas saturation. This change in the drying rate corresponds in the case of dry gas to the advent of a discontinuity and a sharp front on the saturation profile (see Figure 3). In the case of wet gas, profiles (see Figure 5) exhibit a decrease in the water saturation at the outlet of the sample till a uniform saturation is reached all along the sample. The final stage, in the two cases, corresponds to the dry state.

The comparison between experiments 1 and 2 shows clearly the difference between dry gas and humid gas drying effects. Whereas with dry gas it took two hours to dry out the sample, it took ten hours to dry out the sample with humid gas. However, the major difference is observed in the saturation profiles. In the case of dry gas, the drying front propagates from the inlet toward the outlet while in the case of humid gas drying took place first at the outlet and then propagates to the inlet. The two first order mechanisms involved in those cases are most likely an instantaneous phase equilibrium between gas and water coupled with a capillary equilibrium generated by the gas flow and the water saturation. In the dry gas experiment, drying is activated immediately at the entrance of the sample. However in the case of humid gas, water vaporization is due the pressure drop (i.e., gas expansion) along the sample that allows the gas to uptake more vapor as suggested by [4]. In the two cases, capillary forces helps to redistribute water to compensate for the water under-saturation.

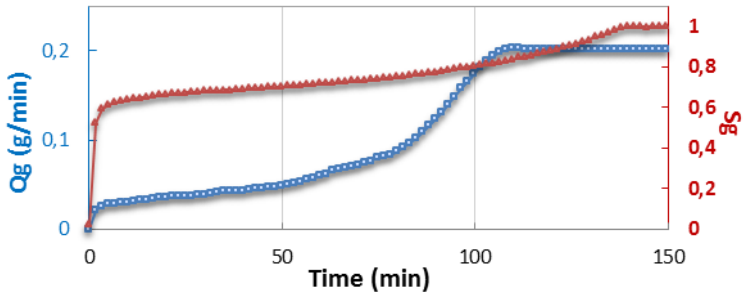

Figure 2: Experiment 1- Gas saturation (red curve) and mass flow rate (blue curve) evolution as a function of time for **dry gas** injection in sample initially saturated with **deionized water**.

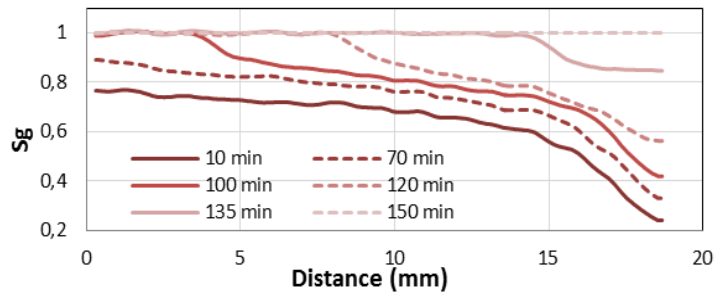

Figure 3: Experiment 1- Evolution of gas saturation profile as a function of time for **dry gas** injection in sample initially saturated with **deionized water** (gas is injected from left).

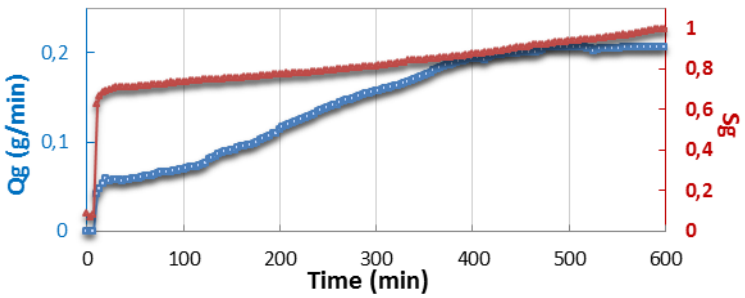

Figure 4: Experiment 2- Gas saturation (red curve) and mass flow rate (blue curve) evolution as a function of time for **humid gas** injection in sample initially saturated with **deionized water**.

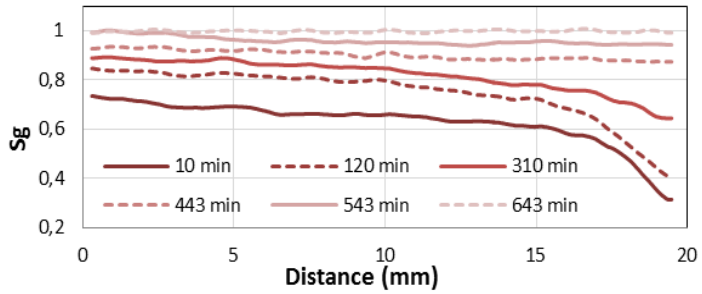

Figure 5: Experiment 2- Evolution of gas saturation profile as a function of time for **humid gas** injection in sample initially saturated with **deionized water** (gas is injected from left).

Effect of salt

In the following experiments, we have injected dry (experiment 3) and humid gas (experiment 4) in a sample initially saturated with a 100g/l KBr brine. Figure 6 and Figure 8 show the evolution of the gas flow rate as a function of time as well as the relative X-ray absorption that was normalized by the finale stage of experiment 3. In the case of dry gas, the flow rate exhibits the same behavior as for the two first experiments. The final flow rate did not show any evidence of permeability alteration due to salt precipitation.

The profiles for the dry gas injection case show a more complex behavior (see Figure 7). The profiles can be interpreted qualitatively as the relative variation in salt quantities (i.e., a relative X-ray absorption above one means a decrease in salt quantity whereas below one means an increase in salt quantity compared to the initial distribution). Thus, we can observe that the salt quantity decreases slightly by the inlet while it increases at a specific location situated 5 mm from the outlet, which corresponds to the location of the capillary end effect. This behavior can be explained by the competition between drying and capillary rise. As drying decreases first the saturation on the side of the inlet as shown by the first experiment, capillary forces tend to equilibrate the saturation by displacing brine toward the inlet. Consequently, the salt concentration increases locally, and once it reaches the solubility limit, it precipitates. However, salt precipitation did not affect the permeability. This is probably due to the low quantity of salt initially present in the sample that represents less than 1% of the pore volume.

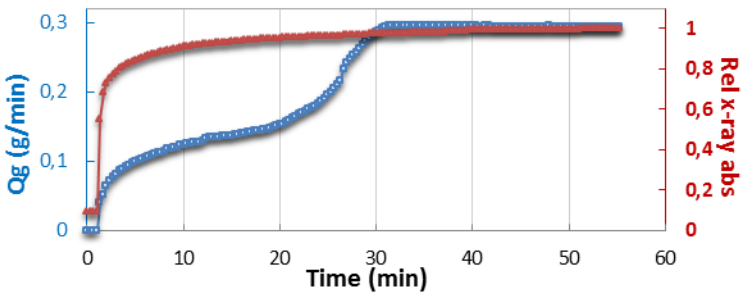

Figure 6: Experiment 3-X-ray relative absorption (red curve) and gas mass flow rate (blue curve) evolution as a function of time for **dry gas** injection in sample initially saturated with 100 g/l KBr **brine**.

.

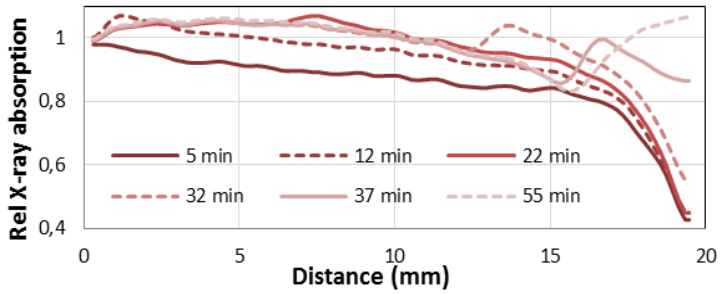

Figure 7: Experiment 3-Evolution of X-ray relative absorption profile as a function of time for **dry gas** injection in sample initially saturated with 100 g/l KBr **brine** (gas is injected from left).

In the case of humid gas injection, the flow rate increases rapidly during the drainage phase before it stabilizes at almost a constant value and remains constant for more than 12 hours. The relative permeability to gas was estimated to 50%, suggesting that the sample had not dried out. The dependency of the water vapor pressure to the salt concentration explains the fact that the sample did not dry out completely. The profiles along the sample, as shown in Figure 9, indicate a variation in the local concentration of the salt that reaches a steady configuration. We can observe a concentration gradient at 750 min that is driven by the equilibrium between the pressure drop, brine salinity and water vapor pressure. In this case, the presence of salt inhibits the drying due to the pressure drop. Clearly the pressure gradient is not high enough to compensate for the reduction in the vapor pressure due to the increase in salt concentration.

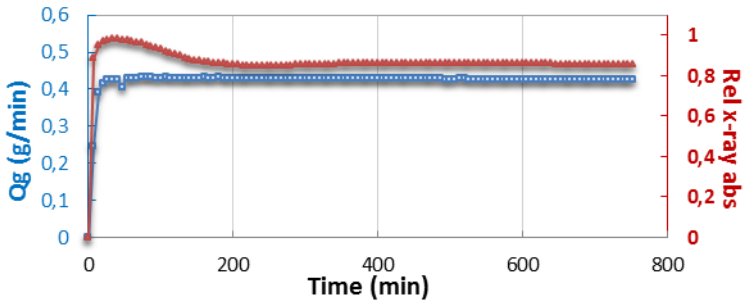

Figure 8: Experiment 4-X-ray relative absorption (red curve) and gas mass flow rate (blue curve) evolution as a function of time for **humid gas** injection in sample initially saturated with 100 g/l KBr **brine**.

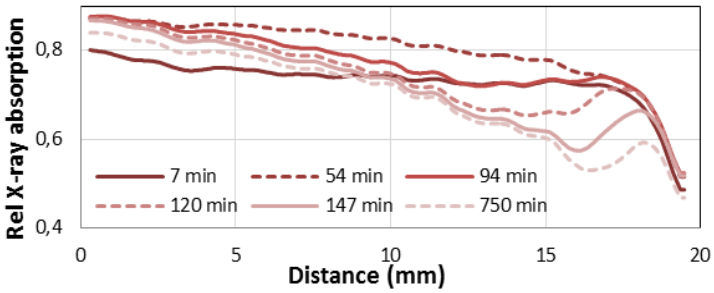

Figure 9: Experiment 4- Evolution of X-ray relative absorption profile as a function of time for **humid gas** injection in sample initially saturated with 100 g/l KBr **brine** (gas is injected from left).

Capillary effect

To investigate the capillary effect, dry gas was injected in a sample initially saturated with a 100g/l KBr brine while contact with brine was maintained by sweeping the bottom face of the sample. Figure 10 shows the evolution of the gas flow rate and the relative X-ray absorption as a function of time. In this case, we observe a completely different behavior than in the previous cases. After an initial increase due to drainage, the gas flow rate experiences successive decline and rise cycles with increasing amplitude before it reaches zero after six hours of injection. The relative X-ray absorption shows a constant decrease which corresponds to an increase of the sample density. This observation suggests an accumulation of additional salt within the sample that is supplied by the brine in contact with the bottom face of the sample.

The profiles illustrated in Figure 11 give more insight into the mechanisms that take place during this experiment. We observe first a local decrease in the relative X-ray attenuation at 8 mm from the inlet at 63 min that suggests an increase in salt concentration. The advent of this salt strip is correlated with a decrease in the gas flow rate and corresponds most probably to salt precipitation that alters permeability to gas. We observe then an alternation of dilutions and precipitation corresponding respectively to the increase and the decline of the gas flow rate with an intensification of the relative X-ray attenuation along the salt strip. Finally, we observe a displacement of the salt strip during the successive cycles of dilution precipitation toward the inlet of the sample. At the end of the experiment the salt strip is located 5 mm far from the inlet.

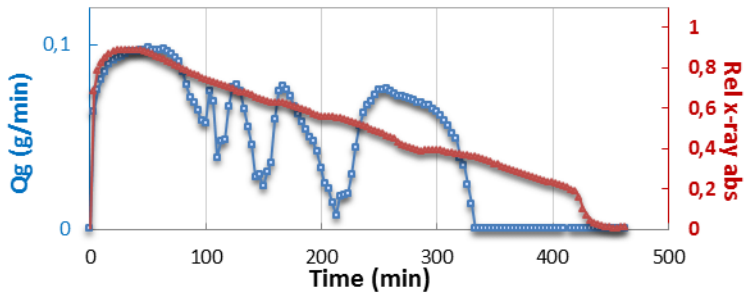

Figure 10: Experiment 5- X-ray relative absorption (red curve) and gas mass flow rate (blue curve) evolution as a function of time for **dry gas** injection in sample initially saturated with 100 g/l KBr **brine** and with **capillary contact**.

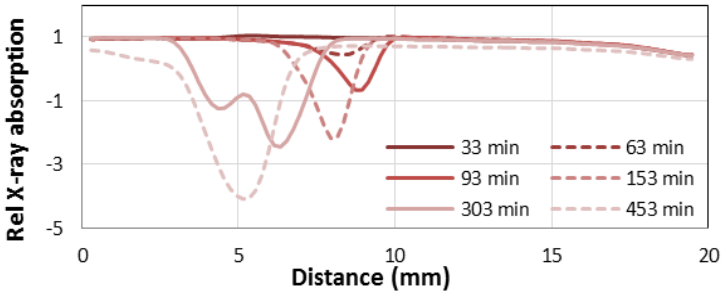

Figure 11: Experiment 5- Evolution of X-ray relative absorption profile as a function of time for **dry gas** injection in sample initially saturated with 100 g/l KBr **brine** and with **capillary contact** (gas is injected from left).

The observed phenomena can be explained by the competition between drying and capillary rise. Indeed, the gas flow dries out the sample, which is manifested by a decrease in the water saturation. However, as we have an active capillary contact, capillary suction compensates for the decrease of water saturation to maintain a capillary equilibrium, which in turn leads to an increase of local salt concentration. At one point the salt concentration is sufficiently high to precipitate salt and altering the gas permeability. As the gas flow rate declines, the capillary rise becomes predominant, allowing the dilution of the precipitated salt and a regeneration of the gas permeability. The alternation of this instable equilibrium leads to an increase of the precipitated salt after each stage till a point of no return is reached where the volume of precipitated salt is sufficiently high to stop the gas flow and the capillary suction.

CONCLUSIONS

In this study, we have shown the importance and interplay of different parameters that govern brine drying and salt precipitation. These parameters include: gas relative humidity, pressure drop, brine concentration, capillary forces and vapor partial pressure.

In the case of dry gas injection in a sample saturated with brine, the water is dried out near the inlet of the sample and will lead to pore plugging if there is sufficient capillary induced flow of brine into the area/location in the plug where the drying effect is strongest. The pore plugging will completely block or strongly reduce the rock permeability.

In the case of humid gas injection in a sample saturated with deionized water, the pressure drop along the core induces an increase in the water content in the gas phase towards the outflow end of the core, allowing evaporation of water at the outlet of the sample. However, if the sample is saturated with brine, the increase in local concentration of brine at the outflow end (caused by evaporation due to the pressure drop) reduces the vapor pressure of the water. This, in turn, inhibits dry-out, as the pressure drop is insufficient to evaporate more water, and one is left with a high salinity brine at the outflow end of the core.

We have demonstrated that dry gas injection combined with a capillary water contact can trigger salt precipitation and possibly blocking of the pore space. These experiments establish the basis for simulation models that can be used to integrate the different physical phenomena that take place during water displacement, evaporation and possibly precipitation.

REFERENCES

1. Kleinitz W., Dietzsch G., Köhler M. (2003) Halite scale formation in gas-producing wells; *Trans. IChemE*, 81(A), pp352-358.
2. Aquilina, P. (2012) Impairment of Gas Well Productivity by Salt Plugging: A Review of Mechanisms, Modeling, Monitoring Methods, and Remediation Techniques, paper SPE 158480 prepared for presentation at the SPE Annual Technical Conference and Exhibition, San Antonio, Tx, 8-10 October.
3. Mahadevan J., Sharma M.M., Yortsos Y.C. (2006) Flow-Through Drying of Porous Media; *AiChE Jounral* ; 52(7); pp2367-2380
4. Mahadevan J., Sharma M.M., Yortsos Y.C. (2007) Water removal from porous media by gas injection: experiments and simulation; *Trans.Porous Media*; 66; pp287-309
5. Peysson Y., Bazin B., Magnier C. Kohler E., Youssef S. (2011) Permeability alteration due to salt precipitation driven by drying in the context of CO_2 injection, *Energy Proceedia* (4) p4387-43941
6. Peysson Y., André L, Azaroual M. (2013) Well injectivity during CO_2 storage operations in deep saline aquifers 1: Experimental investigation of drying effects, salt precipitation and capillary forces, *Int. Journal of Greenhouse Gas Control*, 22, pp 291-300
7. Youssef S., Mascle M., Peysson Y., Olga Vizika O. (2017) CAL-X: an X-Ray Radiography tool for high throughput coreflood experimentation. Applications in the EOR context. To be presented at Int. Sym. of the Society of Core Analyst Vienna, Austria